Analyst

Accepted Manuscript

ROYAL SOCIETY OF CHEMISTRY

www.rsc.org/analyst

TOC:

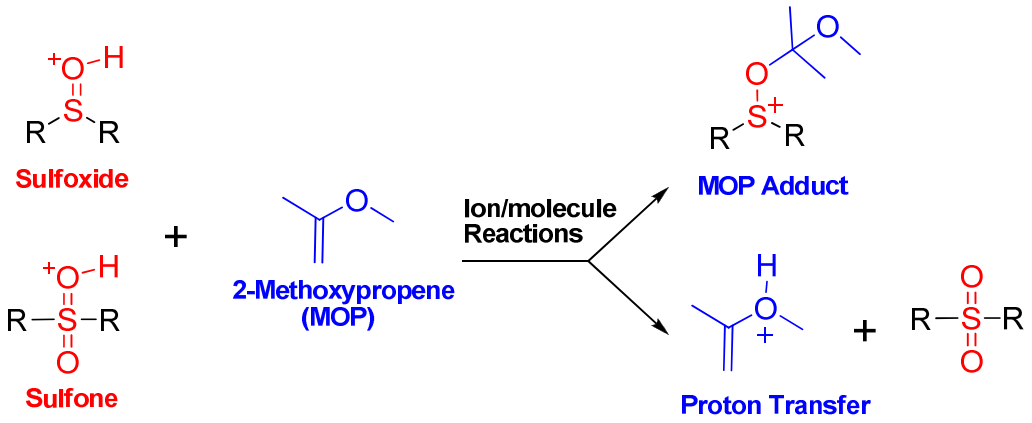

A mass spectrometric method utilizing gas-phase ion/molecule reactions of 2-methoxypropene (MOP) has been developed for the identification of the sulfoxide functionality in protonated analytes in a LQIT mass spectrometer.

Identification of the Sulfoxide Functionality in Protonated Analytes via Ion/molecule Reactions in Linear Quadrupole Ion Trap Mass Spectrometry

Huaming Sheng,[a] *Peggy E. Williams,*[a] *Weijuan Tang,*[a] *Minli Zhang,*[b] *Hilkka I. Kenttämaa*,*[a]

[a]PurdueUniversity, Department of Chemistry, West Lafayette, IN 47907 and

[b]AstraZeneca, Boston, MA 02130

e-mail: hilkka@purdue.edu

Abstract

A mass spectrometric method utilizing gas-phase ion/molecule reactions of 2-methoxypropene (MOP) has been developed for the identification of the sulfoxide functionality in protonated analytes in a LQIT mass spectrometer. Protonated sulfoxide analytes react with MOP to yield an abundant addition product (corresponding to 37 - 99% of the product ions), which is accompanied by a much slower proton transfer. The total efficiency (percent of gas-phase collisions leading to products) of the reaction is moderate (3 – 14%). A variety of compounds with different functional groups, including sulfone, hydroxylamino, N-oxide, aniline, phenol, keto, ester, amino and hydroxy, were examined to probe the selectivity of this reaction. Most of the protonated compounds with proton affinities lower than that of MOP react mainly via proton transfer to MOP. The formation of adduct-MeOH ions was found to be characteristic for secondary *N*-hydroxylamines. N-oxides formed abundant MOP adduct just like sulfoxides, but sulfoxides can be differentiated from N-oxides based on their high reaction efficiencies. The reaction was tested by using the anti-inflammatory drug sulindac (a sulfoxide) and its metabolite sulindac sulfone. The presence of a sulfoxide functionality in the drug but a sulfone functionality in the metabolite was readily demonstrated. The presence of other functionalities in addition to sulfoxide in the analytes was found not to influence the diagnostic reactivity.

1. Introduction

The *in vivo* biotransformation of sulfur atom into sulfoxide is an important oxidation pathway for many sulfur-containing drugs.[1-4] However, the identification of sulfoxides in mixtures can be challenging for many analytical methods, such as NMR, FT-IR and X-ray crystallography, which require relatively large amounts of high-purity analytes.[5-7] Tandem mass spectrometry is a sensitive technique well-suited for obtaining structural information for organic compounds in mixtures. The experiments typically involve ionization of the analyte by protonation followed by the mass-selection of the protonated analyte and its characterization by techniques such as collision-activated dissociation (CAD).[8] However, only a few CAD studies of ionized sulfoxides have been published,[9-11] and none of them show sulfoxide-specific fragmentation patterns. Moreover, the *in vivo* biotransformation of certain drugs can lead to both nitrogen and sulfur oxidation metabolites, which have the same elemental composition and hence cannot be distinguished using high-resolution mass spectrometry.[12]

Tandem mass spectrometric methods based on ion/molecule reactions hold great promise for being able to provide information useful in the identification of specific functional groups in small organic molecules and biomolecules and differentiation of isomers.[13-21] This can be done on analytes as they elute from an HPLC. [22,23] In the work presented here, gas-phase ion/molecule reactions of 2-methoxypropene (MOP) are demonstrated to allow the identification of protonated sulfoxide functionality among many other functional groups, such as sulfone, hydroxylamino, N-oxide,

aniline, phenol, keto, ester, amino and hydroxy functionalities. The potential application of this method to pharmaceuticals is demonstrated by establishing the site of oxygenation to the sulfoxide functionality of a metabolite of the anti-inflammatory drug sulindac.

2. Experimental section

2.1 Chemicals.

Sulindac and sulindac sulfone (purities ≥ 99%) were purchased from VWR. All other chemicals were purchased from Sigma-Aldrich with the purities ≥ 98%. All chemicals were used without further purification.

2.2 Instrumentation

All mass spectrometry experiments were performed using a Thermo Scientific LTQ linear quadrupole ion trap (LQIT) equipped with an APCI source. Sample solutions were prepared in methanol at analyte concentrations ranging from 0.01 up to 1 mg/mL. An integrated syringe drive directly infused the solutions into the APCI source at a rate of 20 μL/min. In the APCI source (operated in positive ion mode), the vaporizer and capillary temperatures were set at 400 °C and 265 °C, respectively. The sheath gas (N_2) flow was maintained at about 30 arbitrary units. The voltages for the ion optics were optimized for each analyte by using the tune feature of the LTQ Tune Plus interface. The detection mass range was from m/z 50 up to 500. The manifold used to introduce reagents into the helium buffer gas line was first described by

Gronert.[24, 25] A diagram of the exact manifold used in this research was published by Habicht et al.[15] MOP was introduced into the manifold via a syringe pump at the rate of 0.17 μL/min. A known amount of He (13 ml/min) was used to dilute MOP. The syringe port and surrounding area were heated to ~70 °C to ensure evaporation of MOP. Before entering the trap, the He/reagent mixture was split using two Granville-Phillips leak valves, instead of the standard flow splitter. This allowed a better control over the amount of the mixture introduced into the instrument. One leak valve was set to establish a helium pressure of ~3 mTorr in the ion trap by allowing ~2 mL/min of the mixture into the trap[26] while the other leak valve controlled the amount of flow diverted to waste. A typical nominal pressure of MOP in the trap during the experiments was 0.68×10^{-5} Torr. After the experiments were completed each day, the manifold was isolated from the instrument and placed under vacuum to remove any remaining reagent.

2.3 Kinetics

After the analytes were ionized by protonation in the APCI source as described above, the protonated analytes were isolated by ejecting all unwanted ions from the trap. An isolation window of two *m/z*-units was employed. The isolated ions were allowed to react for variable time periods (varying residence times in the ion trap) with the reagent MOP introduced as described above. During ion/molecule reactions, the neutral reagent is always present at a constant pressure and its concentration is in excess of that of the ion of interest. Hence, these reactions follow pseudo-first-order

kinetics. The reaction efficiencies (Eff.= $k_{reaction}/k_{collision}$ = the fraction of ion/molecule collisions that results in the formation of products) were determined by measuring each reaction's rate (IM) and the rate of the highly exothermic proton-transfer reaction (PT) between protonated methanol and the reagent (MOP) under identical conditions in the same day. The rates were measured by determining the relative abundances of the reactant ion and product ions as a function of reaction time. The slope of the decay of the reactant ion in a semilogarithmic plot of the ion abundances as a function of time gives the rate constant k multiplied by the concentration of the neutral reagent. Assuming that the exothermic proton-transfer reaction (PT) between protonated methanol and the reagent (MOP) proceeds at collision rate ($k_{collision}$; this can be calculated by using a parameterized trajectory theory[27]), the efficiencies of the ion/molecule reactions can be obtained by using eq 1. This equation is based on the ratio of the slopes of the two reactions studied ($k_{reaction}$[MOP] = slope (IM) and $k_{collision}$[MOP] = slope (PT); the use of the ratio of slopes eliminates the need to know [MOP]), as well as masses of the ion (M_i), neutral reagent (M_n), and methanol ($M_{(PT)}$), and the pressure read by an ion-gauge for the neutral reagent during the ion/molecule reaction ($P_{n(IM)}$) and the proton-transfer reaction ($P_{n(PT)}$).

$$\text{Efficiency} = \frac{\text{slope (IM)}}{\text{slope (PT)}} * \left(\frac{M_i(M_{(PT)}+M_n)}{M_{(PT)}(M_i+M_n)} \right)^{1/2} * \left(\frac{P_{n(PT)}}{P_{n(IM)}} \right) * 100 \qquad \textbf{(1)}$$

3. Results and discussion

2-Methoxypropene (MOP) was chosen as the reagent for this study because the proton affinity (PA) of MOP (214 kcal/mol[21]) is very close to the PA of sulfoxides

(215-220 kcal/mol, Table 1). This may lead to proton transfer within the gas-phase reactant collision complex followed by addition of the now neutral analyte to protonated MOP, as described previously for many boron reagents, such as trimethylborate.[14] Such adducts tend to fragment via an intermolecular proton transfer and elimination of a stable neutral molecule,[14] such as methanol for MOP (Scheme 1b). However, the adducts formed between sulfoxides and protonated MOP do not have acidic protons and hence cannot readily dissociate (Scheme 2; Figure 1). This differentiates sulfoxides from sulfones and most other analytes with relatively low proton affinities (193-205 kcal/mol, Table 1) since they will instead transfer a proton to MOP to give the proton transfer products.

Many protonated model compounds with different functional groups, including sulfoxide, sulfone, hydroxylamino, N-oxide, aniline, amino, ester, keto, hydroxy and phenol, were allowed to react with MOP in a linear quadruple ion trap mass spectrometer (LQIT). As shown in Table 1, most protonated sulfoxide model compounds react with MOP at efficiencies of 3-14% by forming an abundant stable adduct, as expected. CAD on the MOP adducts reformed the protonated sulfoxides. The branching ratios (percentages from all products) of the MOP adducts depend on the PA of the analytes. For example, compounds with higher PA than MOP (e.g., butyl sulfoxide and phenyl sulfoxide) showed mainly MOP adduct formation whereas compounds with lower PA showed more proton transfer product (e.g., methyl phenyl sulfoxide; Table 1).

In sharp contrast to sulfoxides, all protonated sulfones studied react with MOP

rapidly (efficiencies 37-88%) via almost exclusive proton transfer. The same was observed for almost all of the other protonated analytes studied (Tables 2 and 3). The one protonated secondary *N*-hydroxylamine studied shows very low reactivity (likely due to its high PA) but the products resemble those observed for protonated sulfoxides: a stable adduct dominates and is accompanied by a minor proton transfer product (Table 2). The same was observed for protonated aliphatic nitrones and aromatic N-oxides, as reported before. However, the reaction efficiencies (0.2-0.4%) of the N-oxides are 10-times lower than for sulfoxides. Therefore, sulfoxides and N-oxides can be distinguished by their reaction efficiencies.

As shown in Scheme 1, at least two mechanisms can lead to formation of an MOP adduct. One is the direct nucleophilic addition of MOP to the analyte ion (e.g., protonated pyridine N-oxides forms an adduct this way; Scheme 1a). The adduct formation via this mechanism is independent of the PA of the analytes since proton transfer does not take place.[21] Another mechanism involves proton transfer followed by nucleophilic addition by the analyte to protonated MOP (e.g., protonated o-phenylenediamine forms an adduct this way; Scheme 1b). The efficiency of adduct formation via this mechanism is closely related to the PA of the analytes.[19] In the case of sulfoxides, an adduct is proposed to form through the proton transfer / addition mechanism (Scheme 2) since the reaction depends on the PA of the sulfoxide (Tables 1 and 2). For example, protonated diphenyl sulfoxide shows more addition product than protonated methyl phenyl sulfoxide with a lower PA. A protonated N-monosubstituted hydroxylamine yields an adduct that has lost methanol. However,

the N,N-disubstituded hydroxylamine shows the adduct (Table 2). A detailed discussion on these findings will be provided in a separate publication.

Finally, the anti-inflammatory drug sulindac and its metabolite sulindac sulfone were examined. As shown in Figure 1 and Table 1, the site of oxygenation can be easily determined based on their reactions with MOP. The protonated sulfone reacts predominantly by proton transfer while the protonated sulfoxide shows a major stable adduct, as expected. The presence of a carboxylic acid functionality in these analytes does not influence their reactivity toward MOP.

4. Conclusions

The ability to use functional group-selective ion/molecule reactions in a linear quadrupole ion trap mass spectrometer to identify protonated compounds with the sulfoxide functionality has been demonstrated. All protonated sulfoxide model compounds were found to react with MOP to form an abundant stable adduct at efficiencies 3-14%. Protonated N-oxides and N,N-diethyl hydroxylamine react similarly but 10 times slower than protonated sulfoxides. All other compounds studied have substantially lower PA than MOP and hence react rapidly via proton transfer. The results obtained for sulindac and sulindac sulfone suggest that this method is applicable to sulfone containing drugs and drug metabolites even in the presence of other functionalities.

References

1 T. C. Lourenco, J. M. Batista, Jr., M. Furlan, Y. He, L. A. Nafie, C. C. Santana and Q. B. Cass, *J Chromatogr. A* 2012, **1230**, 61-65.

2 Paredes, T. de Campos Lourenco, M. Marzal, A. Rivera, P. Dorny, S. Mahanty, C. Guerra-Giraldez, H. H. Garcia, T. E. Nash and Q. B. Cass, *Antimicrob. Agents Chemother.* 2013, **57**, 944-949.

3 F. I. Zuniga, D. Loi, K. H. Ling and D. D. Tang-Liu, *Expert Opin. Drug Metab. Toxicol.* 2012, **8**, 467-485.

4 X. Chen, S. Hussain, S. Parveen, S. Zhang, Y. Yang and C. Zhu, *Curr. Med. Chem.* 2012, **19**, 3578-3604.

5 J. Caslavska and W. Thormann, *J. Chromatogr. A.* 2011, **1218**, 588-601.

6 D. P. Bhave, W. B. Muse, 3rd and K. S. Carroll, *Infect. Disord. Drug Targets* 2007, **7**, 140-158.

7 D. A. Dibbern, Jr. and A. Montanaro, *Ann. Allergy Asthma Immunol.*, 2008, **100**, 91-100.

8 R. G. Cooks, K. L. Busch and G. L. Glish, *Science* 1983, **222,** 273-291.

9 J. M. Froelich and G. E. Reid, *J. Am. Soc. Mass Spectrom.* 2007, **18**, 1690-1705.

10 G. E. Reid, K. D. Roberts, E. A. Kapp and R. I. Simpson, *J. Proteome Res.* 2004, **3**, 751-759.

11 X. Jiang, J. B. Smith and E. C. Abraham, *J. Mass Spectrom.* 1996, **31**, 1309-1310.

12 H. Kanazawa, A. Okada, Y. Matsushima, H. Yokota, S. Okubo, F. Mashige and K. Nakahara, *J Chromatogr A.* 2002, 949, 1-9.

13 See, for example: (a) S. Osburn and V. Ryzhov, *Anal. Chem.* 2013, **85**, 769-778. (b) J.S. Brodbelt, *Chem. Rev.* 1997, **16**, 91-110. (c) M.N. Eberlin, J. Mass Spectrom., 2006, **41**, 141-156.

14 R. J. Eismin, M. Fu, S. Yem, F. Widjaja and H. I. Kenttämaa, *J. Am. Soc. Mass Spectrom.* 2012, **23**, 12-22.

15 S. C. Habicht, N. R. Vinueza, E. F. Archibold, P. Duan and H. I. Kenttämaa, *Anal. Chem.* 2008, **80**, 3416-3421.

16 K. M. Campbell, M. A. Watkins, S. Li, M. N. Fiddler, B. Winger and H. I. Kenttämaa, *J. Org. Chem.* 2007, **72**, 3159-3165.

17 J. Somuramasami, P. Duan, L. Amundson, E. Archibold, B. Winger and H. I. Kenttämaa, *J. Am. Soc. Mass Spectrom.* 2011, **22**, 1040-1051.

18 M. Fu, R. J. Eismin, P. Duan, S. Li and H. I. Kenttämaa, *Int. J. Mass Spectrom.* 2009, **282**, 77-84.

19 M. Fu, P. Duan, S. Li, S. C. Habicht, D. S. Pinkston, N. R. Vinueza and H. I. Kenttämaa, *Analyst* 2008, **133**, 452-454.

20 P. Duan, M. Fu, T. A. Gillespie, B. E. Winger and H. I. Kenttämaa, *J. Org. Chem.* 2009, **74**, 1114-1123.

21 P. Duan, T. A. Gillespie, B. E. Winger and H. I. Kenttämaa, *J. Org. Chem.* 2008, **73**, 4888-4894.

22 S. C. Habicht, N. R. Vinueza, L. M. Amundson and H. I. Kenttämaa, *J. Am. Soc. Mass Spectrom.* 2011, **52**, 520-530.

23 S. C. Habicht, P. Duan, N. R. Vinueza, M. Fu and H. I. Kenttämaa, *J. Pharm. Biomed. Anal.* 2010, **51**, 805-811.

24 S. Gronert, *J. Am. Soc. Mass Spectrom.* 1998, **9,** 845–848.

25 S. Gronert, *Mass Spectrom. Rev.* 2005, **24**, 100-120.

26 J. C. Schwartz, M. W. Senko and J. E. Syka, *J. Am. Soc. Mass Spectrom.* 2002, **13**, 659-669.

27 T. Su and W. J. Chesnavich, *J. Chem. Phys.* 1982, **76**, 5183–5185.

28 E. P. Hunter, S. G. Lias, Proton Affinity Evaluation. In *NIST Chemistry WebBook, NIST Standard Reference Database Number 69*; Linstrom, P. J., Mallard, W. G., Eds.; National Institute of Standards and Technology: Gaithersburg, MD 20899, http://webbook.nist.gov, (retrieved August 10, 2013).

29 http://www.kore.co.uk/paffinities.htm (Accessed on 4/15/2014)

30 H. Sheng, P. E. Williams, W. Tang, M. Zhang and H. I. Kenttämaa, *J. Org. Chem.* 2014, **79**, 2883-2889.

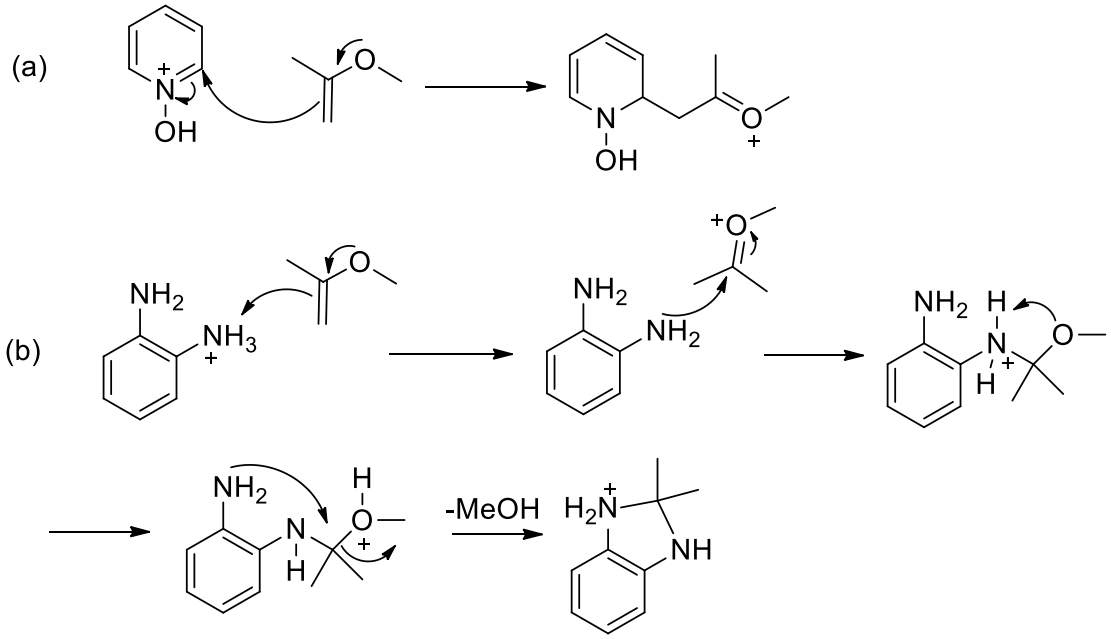

Scheme 1. Published[19,21] mechanisms for the reactions of protonated pyridine N-oxide and protonated o-phenylenediamine with MOP.

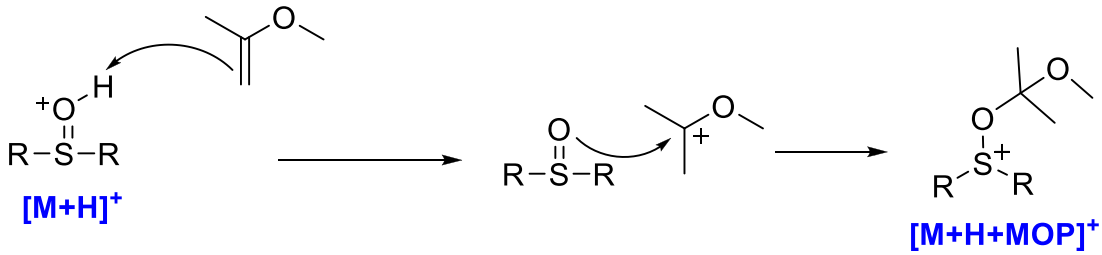

Scheme 2. The mechanism proposed for the formation of a stable adduct between protonated sulfoxide and MOP.

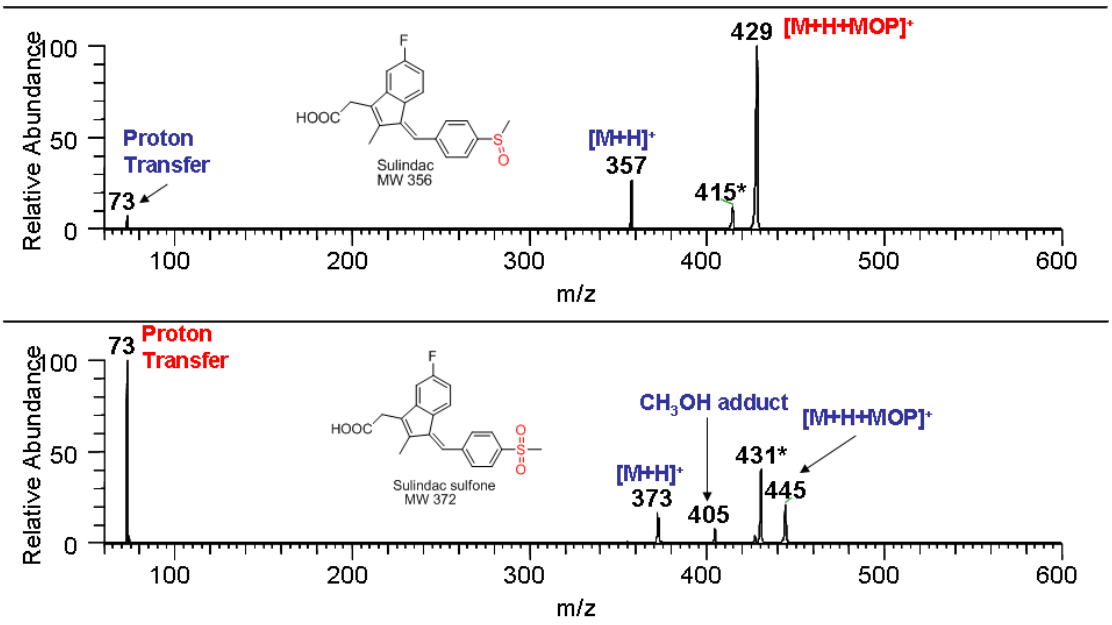

*[M+H+MOP-MeOH+H_2O]+ is formed by water replacing methanol in the ion trap.

Figure 1. An MS/MS mass spectrum measured after 200 ms reaction of protonated sulindac (top) and sulindac sulfone (bottom) with MOP in LQIT. The CH_3OH adduct is formed by solvent addition.

Table 1. Reactions of MOP (PA[a] = 214 kcal/mol) and their efficiencies and different pathways' branching ratios for protonated sulfoxides and sulfones

Reagent (m/z of $[M+H]^+$)	PA[b] (kcal/mol)	Observed reactions and branching ratios		Reaction efficiency[c]
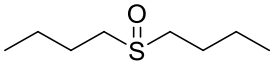 (163)	220.1	Addition Proton transfer	99% 1%	3%
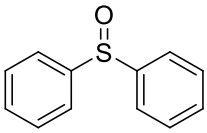 (203)	222.5	Addition Proton transfer	99% 1%	4%
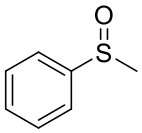 (141)	219.8	Addition Proton transfer	55% 45%	8%
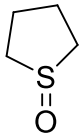 (105)	219.6	Addition Proton transfer	37% 63%	3%
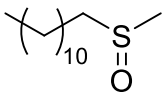 (233)	----	Addition Proton transfer	98% 2%	12%
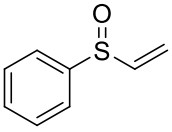 (153)	----	Addition Proton transfer	50% 50%	6%
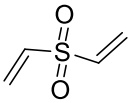 (119)	206.3	Addition Proton transfer	1% 99%	70%
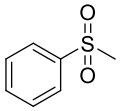 (157)	201.4	Addition Proton transfer	1% 99%	43%
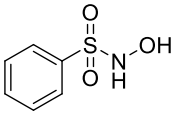 (174)	211.6	Addition Proton transfer	2% 98%	37%

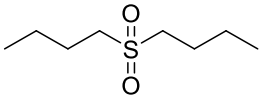 (179)	203.7	Addition Proton transfer	1% 99%	44%
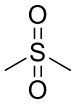 (95)	193.5	Proton transfer	100%	67%
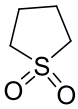 (121)	198.3	Proton transfer	100%	88%
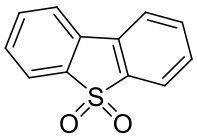 (217)	205.0	Proton transfer	100%	74%
Sulindac (357)	----	Addition Proton transfer	97% 3%	14%
Sulindac sulfone (373)	----	Addition Proton transfer	15% 85%	30%

[a] Reference 21. [b] Reference 30. [c] Precision ± 10%; accuracy ± 50%

Table 2. Reactions of MOP (PA[a] = 214 kcal/mol) and their efficiencies and different pathways' branching ratios for protonated hydroxylamines and N-oxides

Reagent (m/z of $[M+H]^+$)	PA (kcal/mol)	Observed reaction and branching ratios		Reaction efficiency[b]
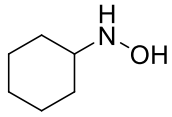 (116)	215.9[c]	Proton transfer Addition–MeOH Addition	51% 25% 24%	5%
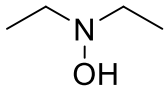 (90)	218.6[d]	Addition Proton transfer	85% 15%	0.2%
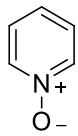 (96)	219.2[c]	Addition Proton transfer	99 % 1%	0.4%
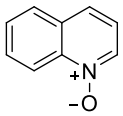 (146)	225.5[e]	Addition Proton transfer	86% 14%	0.3%
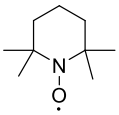 (157)	----	Addition Proton transfer	50% 50%	0.2%
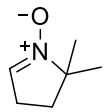 (114)	221.7[a]	Addition Proton transfer	66 % 34%	0.2%

[a] Reference 21. [b] Precision ± 10%; accuracy ± 50% [c] Reference 30.[d] Reference 28. [e] Reference 29.

Table 3. Reactions of MOP (PA [a] = 214 kcal/mol) and their efficiencies and different pathways' branching ratios for protonated carboxylic acid, ketones, ester, phenol and amines

Reagent (m/z of $[M+H]^+$)	PA[b] (kcal/mol)	Observed reaction and branching ratios[c]		Reaction efficiency[c]
Benzoic acid (123)	203.2	Proton transfer	100%	42%
Benzophenone (183)	210.8	Proton transfer Addition	98% 2%	37%
Methyl stearate (299)	------	Proton transfer	100%	76%
Acetone (59)	196.7	Proton transfer	100%	67%
Aniline (94)	210.9	Proton transfer Addition	99.7% 0.3%	10%
Phenol (95)	195.5	Proton transfer Addition	98% 2%	9%
Butylamine (74)	220.2	Proton transfer Addition	98% 2%	0.3%
Butanol (75)	188.8	Proton transfer	100%	87%

[a] Reference 21. [b] Reference 28. [c] Precision $\pm$ 10%; accuracy $\pm$ 50%